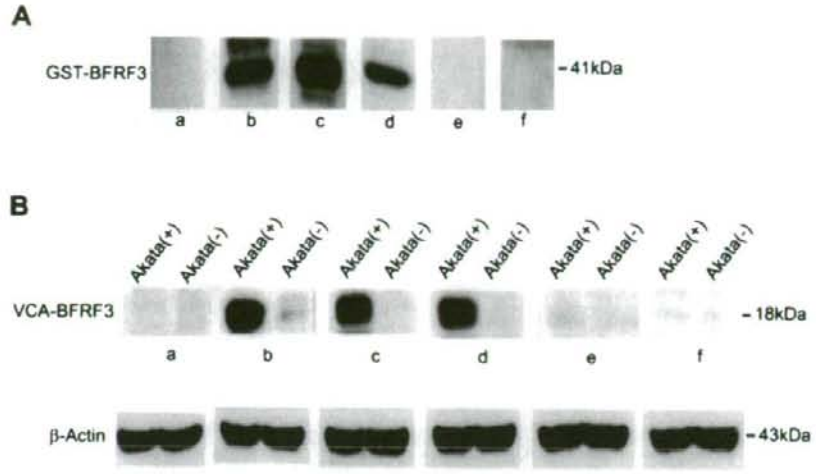

Figure 5. Demonstration of IgM antibody to the Epstein-Barr virus (EBV) BFRF3 protein in the serum of humanized NOG (hNOG) mice. *A*, Immunoblot with the glutathione *s*-transferase (GST)–BFRF3 fusion protein. Purified GST-BFRF3 fusion protein was examined with serum from an EBV-uninfected person *(a)*, an EBV-infected person *(b)*, EBV-infected hNOG mice (*c* and *d*), and an uninfected hNOG mice (*e* and *f*). *B*, Immunoblot with the lysate of EBV-producing Akata cells. Lysate of anti-IgG–treated Akata cells, labeled Akata(+), and of EBV-negative Akata cells, labeled Akata(−), was examined using serum from an EBV-uninfected person *(a)*, an EBV-infected person *(b)*, EBV-infected hNOG mice (*c* and *d*), and uninfected hNOG mice (*e* and *f*).

man T cells). This increase in $CD8^+$ cells were even more conspicuous when their definite number was counted (figure 3*B*). When hNOG mice were inoculated with serially diluted virus samples, a striking dose response was evident; mice inoculated with higher doses exhibited a more profound increase in $CD8^+$ cells at earlier time points (figure 3*C*). Further flow cytometry analyses showed that $CD45RO^+$ memory T cells, compared with $CD45RA^+$ T cells, increased in infected hNOG mice (figure 3*D*). Expression of a T cell activation marker, HLA-DR, was observed mainly in $CD8^+$ cells rather than in $CD4^+$ cells (figure 3*D*).

To demonstrate that these $CD8^+$ T cells were directed against EBV-infected cells, we examined IFN-γ secretion after stimulation with EBV-transformed cells. For this purpose, we first established an LCL using B cells isolated from the same cord blood that was used to isolate HSCs for transplantation. $CD8^+$ T cells, isolated from the peripheral blood of EBV-infected hNOG mice, were incubated with this autologous LCL, and cells secreting IFN-γ were detected by ELISPOT assay. For all 3 EBV-infected hNOG mice (which had been infected at 1×10^3 TD_{50}) thus examined, a significant number of spots were recognized in the wells in which $CD8^+$ T cells were mixed with the autologous LCL, whereas those cells incubated with unrelated LCL had many fewer spots (data from 2 mice are shown in figure 4*A*). $CD8^+$ T cells isolated from uninfected hNOG mice did not give a significant number of spots (data not shown). Release of IFN-γ was blocked by antibody specific to human major histocompatibility complex (MHC) class I but not by that specific to human MHC class II (figure 4*A*). These results clearly show that a T cell response restricted by human MHC class I was mounted against EBV-infected cells. In addition, in 5 of the 6 EBV-infected hNOG mice examined (infected at 1×10^3 TD_{50}), flow cytometry also demonstrated production of IFN-γ by $CD8^+$ T cells isolated from the spleen and stimulated with an autologous LCL (figure 4*B*).

EBV-specific antibody response in hNOG mice. Serum samples from 30 EBV-infected hNOG mice were examined by Western blotting for IgM antibodies reactive with a bacterially expressed GST-BFRF3 fusion protein. The BFRF3 protein is a major component of the virus capsid antigen of EBV [26]. The results are shown in figure 5*A* and indicated that four serum samples (from mice infected at 1×10^1 or 1×10^3 TD_{50}) contained IgM antibody reactive with it. These serum samples reacted also with the 18-kDa BFRF3-encoded protein in the lysate of Akata cells stimulated with IgG antibody to activate virus production (figure 5*B*). Similar experiments with human IgG–specific secondary antibody did not show a positive reaction with either GST-BFRF or $p18^{BFRF3}$. Six serum samples collected from uninfected hNOG mice reacted with neither the 18-kDa protein nor GST-BFRF3 (figure 5 and data not shown). These results indicate that hNOG mice have the ability to mount an IgM response to EBV.

DISCUSSION

The lymphoproliferative disease induced in hNOG mice is remarkably similar to the human lymphoproliferative disorder seen in immunocompromised hosts [27] with respect to histology, surface phenotype, and the type of EBV gene expression

(latency III). Reproduction of latency III in the present study makes for an interesting contrast with the previous model using NOD/*scid* mice, which exhibited the latency II pattern [10].

EBV infection in lower doses resulted in a transient increase in EBV DNA load in the peripheral blood, followed by apparently asymptomatic infection that persisted for at least 22 weeks. This type of asymptomatic EBV infection has not been described in nonprimate models of EBV infection and may be regarded as a model of human EBV latency. To compare this condition in NOG mice with EBV latency in humans precisely, we need to further investigate the nature of host cells (i.e., whether they are memory B cells), the pattern of EBV gene expression in them, and the involvement of anti-EBV immune responses in its maintenance.

In hNOG mice, human T cells develop in thymus tissue, in which epithelial cells are of murine origin [16]. It is therefore interesting that they could mount a T cell response restricted by human MHC class I. Although this suggests that positive selection of human T cells occurred in hNOG mice, the mechanism of T cell education remains unclear. Alloantigen-specific and human MHC class I–restricted T cell cytotoxicity has been reported in hNOG mice [15, 16]. An EBV-induced T cell response was evident in mice that received high doses of virus and developed lymphoproliferative disorder, suggesting that the T cell response in hNOG mice was not sufficient to control EBV-induced lymphoproliferation when they were infected at high doses. That only a minor fraction of $CD8^+$ T cells appeared to be EBV specific, as evidenced by ELISPOT assay and flow cytometry, may explain this result, at least partially. A humoral immune response to EBV has not been documented in previous mouse models of EBV infection, and therefore the NOG mouse may provide a valuable tool to analyze the mechanism and the protective roles of antibody response in EBV infection. We have to date clearly identified only IgM antibody to the 18-kDa component of virus capsid antigen in a minor fraction (4/30) of infected mice. We are currently attempting to improve sensitivity and to see whether hNOG mice can mount a more efficient and divergent antibody response to the virus, possibly including the production of IgG antibodies. Because both the T cell–mediated and the humoral immune response are elicited in hNOG mice, they may be useful in the evaluation of candidate EBV vaccines.

Very recently, humanized mice based on other immunodeficient mouse strains were prepared, and EBV was used as a typical pathogen to analyze their immune functions. Traggiai et al. [12] infected humanized $Rag2^{-/-}$IL-$2R\gamma^{-/-}$ mice with EBV and documented an in vitro proliferative response by $CD8^+$ T cells to an autologous LCL. Melkus et al. [11], on the other hand, humanized NOD/*scid* mice by transplanting human fetal liver, thymus, and HSCs and succeeded in inducing an EBV-specific T cell immune response as well as an innate immune response to toxic shock syndrome toxin 1. These 2 studies were performed mainly using immunological standpoints and did not provide detailed data from virological investigations. An advantage of the NOG mouse model described here is that it does not require a fine surgical procedure using human fetal tissue; therefore, NOG mice can be easily provided in large quantities.

In immunocompromised humans, failure of immunosurveillance may lead to the development of lymphoproliferative disorder. We expect that the NOG mouse model can be used to analyze the exact relationship between immunodeficiency and the development of lymphoproliferative disorder. Immune responses in the hNOG mouse can be modulated by immunosuppressive drugs (such as cyclosporine A) or HIV, and the development of lymphoproliferative disorder can be analyzed with special reference to the nature and level of immunodeficiency. This kind of study, which has not been possible with conventional *scid* mice, may reveal an exact condition in which lymphoproliferative disorder develops and may thereby aid the development of a specified immunosuppressive procedure that evades this condition and precludes the risk of lymphoproliferative disorder.

In summary, the NOG mouse is able to recapitulate various essential elements of human EBV infection and is therefore, to our knowledge, the most comprehensive small-animal model of EBV infection described to date. It should be a valuable tool for the study of the pathogenesis, prevention, and treatment of EBV infection.

Acknowledgments

We thank Satoshi Itakura, Fuyuko Kawano, Eri Yamada, Miki Mizukami, and Ken Watanabe for technical assistance. We thank Shizuko Minegishi for advice on flow cytometry, Atsushi Komano for advise on the enzyme-linked immunospot assay, Ayako Demachi-Okamura and Kiyotaka Kuzushima for advice on detection of Epstein-Barr virus–specific T cells, and Shosuke Imai for helpful discussions. We thank the Tokyo Cord Blood Bank for supplying cord blood.

References

1. Rickinson AB, Kieff E. Epstein-Barr virus. In: Knipe DM, Howley PM, eds. Fields virology. Philadelphia: Lippincott Williams & Wilkins, **2001**: 2575–628.
2. Kieff E, Rickinson AB. Epstein-Barr virus and its replication. In: Knipe DM, Howley PM, eds. Fields virology. 4th ed. Philadelphia: Lippincot Williams & Wilkins, **2001**:2511–74.
3. Young LS, Finerty S, Brooks L, Scullion F, Rickinson AB, Morgan AJ. Epstein-Barr virus gene expression in malignant lymphomas induced by experimental virus infection of cottontop tamarins. J Virol **1989**; 63: 1967–74.
4. Miller G, Shope T, Coope D, et al. Lymphoma in cotton-top marmosets after inoculation with Epstein-Barr virus: tumor incidence, histologic spectrum antibody responses, demonstration of viral DNA, and characterization of viruses. J Exp Med **1977**; 145:948–67.
5. Cho Y, Ramer J, Rivailler P, et al. An Epstein-Barr-related herpesvirus from marmoset lymphomas. Proc Natl Acad Sci USA **2001**; 98:1224–9.
6. Moghaddam A, Rosenzweig M, Lee-Parritz D, Annis B, Johnson RP, Wang F. An animal model for acute and persistent Epstein-Barr virus infection. Science **1997**; 276:2030–3.
7. Mosier DE, Gulizia RJ, Baird SM, Wilson DB. Transfer of a functional human immune system to mice with severe combined immunodeficiency. Nature **1988**; 335:256–9.

8. Okano M, Taguchi Y, Nakamine H, et al. Characterization of Epstein-Barr virus-induced lymphoproliferation derived from human peripheral blood mononuclear cells transferred to severe combined immunodeficient mice. Am J Pathol **1990**; 137:517–22.
9. Rowe M, Young LS, Crocker J, Stokes H, Henderson S, Rickinson AB. Epstein-Barr virus (EBV)-associated lymphoproliferative disease in the SCID mouse model: implications for the pathogenesis of EBV-positive lymphomas in man. J Exp Med **1991**; 173:147–58.
10. Islas-Ohlmayer M, Padgett-Thomas A, Domiati-Saad R, et al. Experimental infection of NOD/SCID mice reconstituted with human CD34+ cells with Epstein-Barr virus. J Virol **2004**; 78:13891–900.
11. Melkus MW, Estes JD, Padgett-Thomas A, et al. Humanized mice mount specific adaptive and innate immune responses to EBV and TSST-1. Nat Med **2006**; 12:1316–22.
12. Traggiai E, Chicha L, Mazzucchelli L, et al. Development of a human adaptive immune system in cord blood cell-transplanted mice. Science **2004**; 304:104–7.
13. Hiramatsu H, Nishikomori R, Heike T, et al. Complete reconstitution of human lymphocytes from cord blood CD34+ cells using the NOD/SCID/γ_c^{null} mice model. Blood **2003**; 102:873–80.
14. Ito M, Hiramatsu H, Kobayashi K, et al. NOD/SCID/γ_c^{null} mouse: an excellent recipient mouse model for engraftment of human cells. Blood **2002**; 100:3175–82.
15. Yahata T, Ando K, Nakamura Y, et al. Functional human T lymphocyte development from cord blood CD34+ cells in nonobese diabetic/Shi-scid, IL-2 receptor gamma null mice. J Immunol **2002**; 169:204–9.
16. Ishikawa F, Yasukawa M, Lyons B, et al. Development of functional human blood and immune systems in NOD/SCID/IL2 receptor γ chain^{null} mice. Blood **2005**; 106:1565–73.
17. Miyazato P, Yasunaga J, Taniguchi Y, Koyanagi Y, Mitsuya H, Matsuoka M. De novo human T-cell leukemia virus type 1 infection of human lymphocytes in NOD-SCID, common gamma-chain knockout mice. J Virol **2006**; 80:10683–91.
18. Watanabe S, Terashima K, Ohta S, et al. Hematopoietic stem cell-engrafted NOD/SCID/IL2Rgamma null mice develop human lymphoid systems and induce long-lasting HIV-1 infection with specific humoral immune responses. Blood **2007**; 109:212–8.
19. Dewan MZ, Terashima K, Taruishi M, et al. Rapid tumor formation of human T-cell leukemia virus type 1-infected cell lines in novel NOD-SCID/gammac^{null} mice: suppression by an inhibitor against NF-kappaB. J Virol **2003**; 77:5286–94.
20. Watanabe S, Ohta S, Yajima M, et al. Humanized NOD/SCID/IL2Rγ^{null} mice transplanted with hematopoietic stem cells under nonmyeloablative conditions show prolonged life spans and allow detailed analysis of human immunodeficiency virus type 1 pathogenesis. J Virol **2007**; 81: 13259–64.
21. Takada K, Ono Y. Synchronous and sequential activation of latently infected Epstein-Barr virus genomes. J Virol **1989**; 63:445–9.
22. Condit RC. Principles of virology. In: Knipe DM, Howley PM, eds. Fields virology. Philadelphia: Lippincott Williams & Wilkins, **2001**:19–51.
23. Kimura H, Morita M, Yabuta Y, et al. Quantitative analysis of Epstein-Barr virus load by using a real-time PCR assay. J Clin Microbiol **1999**; 37:132–6.
24. Nakamura H, Iwakiri D, Ono Y, Fujiwara S. Epstein-Barr-virus-infected human T-cell line with a unique pattern of viral-gene expression. Int J Cancer **1998**; 76:587–94.
25. Kuzushima K, Hoshino Y, Fujii K, et al. Rapid determination of Epstein-Barr virus-specific CD8$^+$ T-cell frequencies by flow cytometry. Blood **1999**; 94:3094–100.
26. van Grunsven WM, Nabbe A, Middeldorp JM. Identification and molecular characterization of two diagnostically relevant marker proteins of the Epstein-Barr virus capsid antigen complex. J Med Virol **1993**; 40: 161–9.
27. Rezk SA, Weiss LM. Epstein-Barr virus-associated lymphoproliferative disorders. Hum Pathol **2007**; 38:1293–304.

STEM CELLS

TISSUE-SPECIFIC STEM CELLS

Quiescent Human Hematopoietic Stem Cells in the Bone Marrow Niches Organize the Hierarchical Structure of Hematopoiesis

TAKASHI YAHATA,[a,b,c] YUKARI MUGURUMA,[a] SHIZU YUMINO,[a] YIN SHENG,[a] TOMOKO UNO,[a] HIDEYUKI MATSUZAWA,[a] MAMORU ITO,[d] SHUNICHI KATO,[a,c] TOMOMITSU HOTTA,[a,b] KIYOSHI ANDO[a,b]

[a]Division of Hematopoiesis, Research Center for Regenerative Medicine; [b]Department of Hematology; [c]Department of Cell Transplantation and Regenerative Medicine; Tokai University School of Medicine, Kanagawa, Japan; [d]Central Institute for Experimental Animals, Kawasaki, Japan

Key Words. Cell cycle • Clonal assays • Hematopoietic stem cell transplantation • Long-term repopulation • Mesenchymal stem cells • Stem cell-microenvironment interactions • Human hematopoietic stem cells • Severe combined immunodeficient repopulating cell

ABSTRACT

Hematopoiesis is a dynamic and strictly regulated process orchestrated by self-renewing hematopoietic stem cells (HSCs) and the supporting microenvironment. However, the exact mechanisms by which individual human HSCs sustain hematopoietic homeostasis remain to be clarified. To understand how the long-term repopulating cell (LTRC) activity of individual human HSCs and the hematopoietic hierarchy are maintained in the bone marrow (BM) microenvironment, we traced the repopulating dynamics of individual human HSC clones using viral integration site analysis. Our study presents several lines of evidence regarding the in vivo dynamics of human hematopoiesis. First, human LTRCs existed in a rare population of CD34 CD38 cells that localized to the stem cell niches and maintained their stem cell activities while being in a quiescent state. Second, clonally distinct LTRCs controlled hematopoietic homeostasis and created a stem cell pool hierarchy by asymmetric self-renewal division that produced lineage-restricted short-term repopulating cells and long-lasting LTRCs. Third, we demonstrated that quiescent LTRC clones expanded remarkably to reconstitute the hematopoiesis of the secondary recipient. Finally, we further demonstrated that human mesenchymal stem cells differentiated into key components of the niche and maintained LTRC activity by closely interacting with quiescent human LTRCs, resulting in more LTRCs. Taken together, this study provides a novel insight into repopulation dynamics, turnover, hierarchical structure, and the cell cycle status of human HSCs in the recipient BM microenvironment. STEM CELLS *2008;26:3228–3236*

Disclosure of potential conflicts of interest is found at the end of this article.

INTRODUCTION

One of the essential features of hematopoietic stem cells (HSCs) is their ability to remain in a quiescent state to maintain long-term repopulating activity [1]. Regulatory mechanisms that govern this quiescent state are crucial for organizing the hierarchical structure of hematopoiesis and are also of critical biological importance in preventing premature HSC exhaustion under conditions of hematopoietic stress. Several murine studies have demonstrated that interactions between HSCs and stem cell niches, specialized bone marrow (BM) microenvironments created by supporting cells, via receptor-ligand interactions and cell-adhesion molecules expressed in both cell types play central roles in regulating stem cell properties [2]. At present, at least two distinct niches have been identified in the endosteal areas of BM: the osteoblastic niche and the vascular niche [3–5]. However, it remains unclear whether these principles of the niche-HSC regulatory system, extrapolated from murine studies, could apply to human situations.

The severe combined immunodeficient (SCID) mouse-repopulating cell (SRC) assay is considered to be the most reliable research tool for in vivo analysis of the biological processes of human hematopoiesis [6]. In this assay system, SRCs, defined by their ability to reconstitute human hematopoiesis in immunodeficient mice, can be classified into several subtypes on the basis of the lineage restriction of their progenies and the timing of their appearance after transplantation. Although long-term repopulating cell (LTRC) activities with lymphomyeloid potential are mostly restricted to the CD34 CD38^{low} population, the CD34 CD38 population exhibits only short-term repopulating cell (STRC) activities [7–9]. STRCs are further subdivided into myeloid-restricted STRCs (STRC-Ms) and lymphomyeloid STRCs (STRC-MLs) [10]. The hierarchical relationships of each SRC pop-

Author contributions: T.Y.: conception and design, collection and assembly of data, data analysis and interpretation, and manuscript writing; Y.M.: collection and assembly of data, data analysis and interpretation, and manuscript writing; S.Y., Y.S., T.U., and H.M.: collection of data; M.I., S.K.: provision of study material; T.H. and K.A.: conception and design, financial support, and final approval of manuscript.

Correspondence: Kiyoshi Ando, M.D., Ph.D., Division of Hematopoiesis, Research Center for Regenerative Medicine and Department of Hematology, Tokai University School of Medicine, 143 Shimokasuya, Isehara, Kanagawa 259-1193, Japan. Telephone: 81-463-93-1121; Fax: 81-463-92-4511; e-mail: andok@keyaki.cc.u-tokai.ac.jp Received June 11, 2008; accepted for publication September 3, 2008; first published online in STEM CELLS *EXPRESS* September 11, 2008. 1066-5099/2008/$30.00/0 doi: 10.1634/stemcells.2008-0552

ulation and the precise characteristics regarding functions of individual human HSCs remain elusive.

Clonal analysis of the unique proviral integration sites is a powerful approach to identify and trace the activity of individual SRCs for comprehensive understanding of the properties of individual HSCs [11]. Random and permanent integration of virus vectors into the host cell genome makes the vector-genomic DNA junction a unique marker by which to identify the originally transduced cells and their progenies. By combining lineage-cell sorting and a linear amplification-mediated (LAM)-polymerase chain reaction (PCR) technique that verifies individual proviral integration into the human genome by direct sequence, we have developed a strategy by which to examine the multipotency of a single human HSC from two angles [12]. First, clonal analysis of each lineage cell proves the presence of the repopulating cell, which is the ancestor of the currently analyzed lineage cell (retrospective identification). Second, the stem cell phenotype and the capacity of individual SRC clones at the time of analysis distinguish self-renewing clones and differentiating clones (current status identification). Using this approach, we have recently documented heterogeneity among individual SRC clones regarding their stem cell activity, differentiation potential, and clonal longevity within the stem cell pool [12].

In this study, we investigated the in vivo repopulating dynamics of 228 sequence-verified individual SRC clones with respect to differentiation potential, self-renewal capacity, and cell cycle status in the niche. We successfully identified human LTRCs that were responsible for lifelong hematopoiesis in the BM microenvironment. Those human LTRCs localized to and interacted with the key components of the stem cell niche in a quiescent state. Once activated, they divided into LTRCs and STRCs by asymmetric self-renewal division, ultimately creating a hierarchical hematopoietic structure.

MATERIALS AND METHODS

Collection and Fractionation of Cord Blood CD34 Cells

Cord blood (CB) samples were obtained from full-term deliveries according to the institutional guidelines approved by the Tokai University Committee on Clinical Investigation. CD34 cell fractions were prepared using the CD34 Progenitor Cell Isolation Kit (Miltenyi Biotec, Sunnyvale, CA, http://www.miltenyibiotec.com). Pooled CD34 -enriched cells from multiple donors were stained with allophycocyanin (APC)-conjugated anti-lineage-specific antigens CD3 (UCHT1), CD41 (P2), glycophorin A (11E4B-7-6) (all from Coulter/Immunotech, Marseille, France), CD14 (MfP9), CD19 (SJ25C1), and CD56 (NCAM16.2) (all from BD Biosciences, San Jose, CA, http://www.bdbiosciences.com) and with phycoerythrin (PE)-conjugated anti-CD38 (HB7; BD Biosciences) and fluorescein isothiocyanate (FITC)-conjugated anti-CD34 (581; Beckman Coulter, Fullerton, CA, http://www.beckmancoulter.com) monoclonal antibodies. Cells were gated on lineage marker-negative and/or low-expression region, and Lin ^{low}CD34 cells were fractionated according to their CD38 expression levels using the FACSVantage flow cytometer (BD Biosciences). To eliminate the contamination of each subpopulation, we performed two consecutive rounds of cell sorting to ensure more than 99% cell purity.

Lentivirus Infection

Fractionated CD34 cells were plated on fibronectin CH-296 fragment (Takara Shuzo, Shiga, Japan, http://www.takara-bio.co.jp) and incubated with highly concentrated viral supernatant at a multiplicity of infection of 50 in serum-free StemPro-34 medium (Invitrogen, Carlsbad, CA, http://www.invitrogen.com) containing the following cytokines for 16 hours: recombinant human thrombopoietin (50 ng/ml; kindly donated by Kirin Brewery Co., Tokyo, http://www.kirin.co.jp/english), stem cell factor (50 ng/ml; donated by Kirin Brewery), and Flk-2/Flt-3 ligand (50 ng/ml; R&D Systems Inc., Minneapolis, http://www.rndsystems.com). The infection efficiency was 72.4% 8.5%.

Human Hematopoietic Repopulation

NOD/Shi-scid, IL-2R c^{null} (NOG) mice were obtained from the Central Institute for Experimental Animals (Kawasaki, Japan) and maintained in the animal facility of the Tokai University School of Medicine in microisolator cages; the animals were fed with autoclaved food and water. This strain exhibits a high engraftment rate of human hematopoietic cells than other existing strains such as NOD/SCID and NOD/SCID/ 2m^{null}, allowing the reconstitution capacity and lymphomyeloid differentiation of human repopulating stem cells to be assessed [13, 14]. Nine- to 20-week-old NOG mice were irradiated with 250 cGy of x-rays. The following day, transduced cells were injected into the retro-orbital plexus of the NOG mice. At the indicated times after transplantation, the mice were humanely killed, and BM cells, splenocytes, and thymocytes were harvested. Human hematopoietic cells were distinguished from mouse cells by the expression of human CD45. Enhanced green fluorescent protein (EGFP)-expressing CD45 human hematopoietic cells were further classified into human stem/progenitor (CD34), myeloid (CD33), B-lymphoid (CD19), and T-lymphoid (CD3 or CD4 /CD8) subpopulations and were sorted using a FACSVantage Diva option (BD Biosciences). Sorted populations had purities of more than 99%. All experiments were approved by the animal care committee of Tokai University.

Secondary Transplantation

BM cells were obtained from mice transplanted with CD34 CD38^{neg} cells at 18 weeks after transplantation, and CD34 cells were isolated by cell sorting. Purified CD34 cells of the primary recipients were divided in half and injected intravenously into two sublethally irradiated secondary NOG recipients (1.5 10^6 cells per recipient). One recipient was sacrificed at 3 weeks and the other at 18 weeks after transplantation. BM cells and thymocytes were collected from each secondary recipient and used for flow cytometric analysis and lineage cell sorting as described earlier.

Integration Site Analysis of Lentivirally Marked SRCs

Genomic DNA isolation and LAM-PCR were carried out as described previously [12]. The proviral integration sites of CD33 cells were sequenced, and the sequences were examined for alignment to the human genome using NCBI BlastN (http://www.ncbi.nlm.nih.gov/blast). The verified genomic sequence information of these CD33 cell integration sites was used to design new primers (all primer sequences used in this study are listed in supplemental online Tables 1 and 2). PCR was performed on each LAM-PCR product using the unique genomic flanking primers.

Estimation of Clone Size by Real-Time Quantitative PCR

The relative clone size of individual LTRC clones that was detected in the CD34 cells of primary and secondary recipients was examined as described previously [12]. For real-time quantitative PCR, each target DNA was amplified on the same plate, with -globin as the reference, using the QuantiTect SYBR Green PCR Master Mix (Qiagen, Hilden, Germany, http://www1.qiagen.com) and the ABI Prism 7700 Sequence Detection System (Applied Biosystems, Foster City, CA, http://www.appliedbiosystems.com). The relative clone amounts and range were determined in reference to -globin. A comparative threshold cycle (C_T) was used to determine the proportion of CD34 clones in paired recipients. For each sample, the clone C_T value was normalized using the formula C_T $C_{T\ clone}$ $C_{T\ \text{-globin}}$. To determine relative clone size, the following formula was used: C_T $C_{T\ clone}$ in CD34 cells of the primary recipient $C_{T\ clone}$ in CD34 cells of the secondary

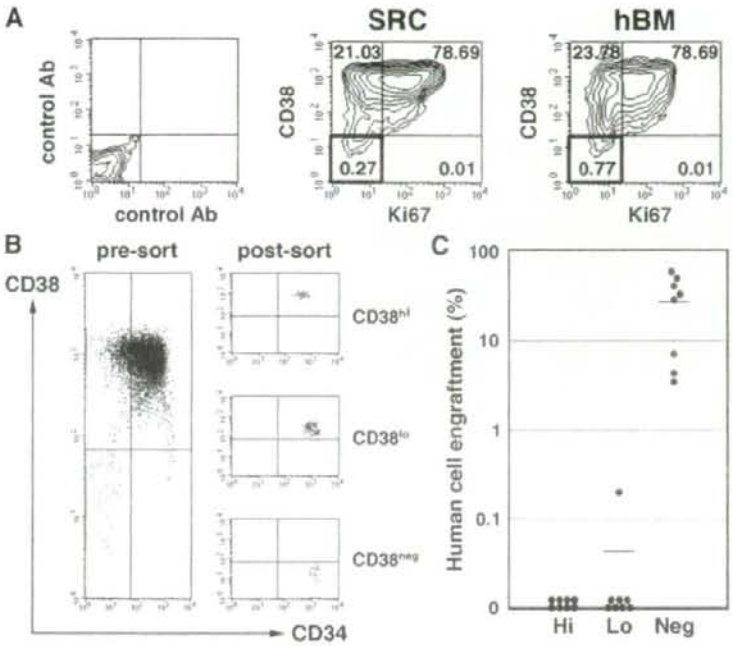

Figure 1. Cell cycle status and stem cell activity of CD34 cells. **(A):** Bone marrow (BM) CD34 cells were analyzed for their expression of CD38 and Ki-67 by flow cytometry. Representative fluorescence-activated cell sorting profiles of isotype control: CD34 cells in the NOD/Shi-scid, IL-2R c^{null} (NOG) recipient BM; and freshly isolated hBM CD34 cells from five independent experiments are shown. The relative frequencies of each population are indicated. **(B):** Representative sorting profiles of CD34 cells obtained from primary recipient BM. Fractionated CD34 cells were transplanted into secondary NOG hosts (CD34 $CD38^{neg}$, 1–7 10^5 cells; CD34 $CD38^{lo}$, 1–3.5 10^5 cells; CD34 $CD38^{hi}$, 5–8 10^5 cells). **(C):** Secondary recipient BM cells were analyzed for the expression of human CD45. Each symbol represents one mouse, and horizontal bars indicate the average engraftment level in three independent experiments. Abbreviations: Ab, antibody; hBM, human bone marrow; Hi, high; Lo, low; Neg, negative; SRC, severe combined immunodeficient mouse-repopulating cell.

recipient. The value was calculated by the expression 2 ^{C_T}. Each reaction was performed at least in triplicate.

Cell Cycle Analysis

CD34 BM cells were stained with PE-conjugated anti-CD38 and APC-conjugated anti-CD34 antibodies. The cells were then fixed and permeabilized using a Cell Permeabilization Kit (BD Biosciences) and stained with FITC-conjugated anti-Ki-67 antibody (BD Biosciences). Fluorescence-activated cell sorting analysis was performed on a FACSCalibur using CELLQuest software (BD Biosciences).

Histological Analysis of BM Microenvironment

Tissue processing and immunofluorescent staining were performed as described previously [15]. For in situ examination of transplanted nonhematopoietic human cells, genetically EGFP-marked human mesenchymal stem cells (MSCs) were transplanted directly into the right tibias of NOG mice. The following antibodies were used for tissue immunostaining: anti-human CD34 (My10; BD Biosciences), anti-human CD38 (HI12; BD Biosciences), anti-human CD31 (TECHNE, Minneapolis, http://www.techne-corp.com), anti-human SDF-1 (Santa Cruz Biotechnology Inc., Santa Cruz, CA, http://www.scbt.com), and anti-proliferating cell nuclear antigen (anti-PCNA; Abcam, Cambridge, U.K., http://www.abcam.com). Immunofluorescent-stained slides were examined, and images were captured using an LSM510 META confocal microscope (Carl Zeiss, Jena, Germany, http://www.zeiss.com). Images were processed by Adobe Photoshop 7.0 (Adobe Systems Inc., San Jose, CA, http://www.adobe.com).

Statistical Analysis

Data are represented as mean SD. p values .05 were considered to be significant.

RESULTS

Only Quiescent CD34 $CD38^{neg}$ Cells in the Recipient Sustain Long-Term Hematopoiesis

To investigate the characteristics of human LTRCs in the recipient BM, we transplanted CB CD34 $CD38^{neg}$ cells into sublethally irradiated NOG mice. Eighteen weeks after transplantation, we examined the cell cycle status and repopulating ability of engrafted CD34 cells in recipient BM. $CD38^{neg}$ cells accounted for a very small population of CD34 cells in the BM of transplanted mice (1.33% 1.18%; n 7). The expression of Ki-67, a nuclear protein expressed during all active parts of the cell cycle in proliferating cells, was examined to evaluate the cell cycle status of CD34 cells in the BM of transplanted mice. Although a majority of CD34 CD38 cells expressed Ki-67, less than 0.1% of CD34 $CD38^{neg}$ cells were positive for Ki-67 (Fig. 1A), confirming that CD34 $CD38^{neg}$ cells in the recipient BM were indeed dormant. Interestingly, the cell surface phenotype, high levels of CD38 expression in the majority of CD34 cells, and the cell cycle status of CD34 cells in the NOG mice closely resembled those of human BM-derived CD34 cells (Fig. 1A), suggesting that the human BM microenvironment of NOG mouse can substitute, at least in part, for the function of a human BM microenvironment.

To examine the LTRC activity of CD34 cells in recipient BM, we separated CD34 cells into $CD38^{neg}$, $CD38^{lo}$, and $CD38^{hi}$ fractions and transplanted these fractions into secondary NOG hosts (Fig. 1B). Secondary transplantable LTRCs were found almost exclusively in the extremely rare fraction of CD34 $CD38^{neg}$ cells (Fig. 1C). These cells were able to display multilineage engraftment in secondary recipients (supplemental online Fig. 1). Our results revealed that CD34 $CD38^{neg}$ cells in recipient BM stayed in the quiescent state and that only these

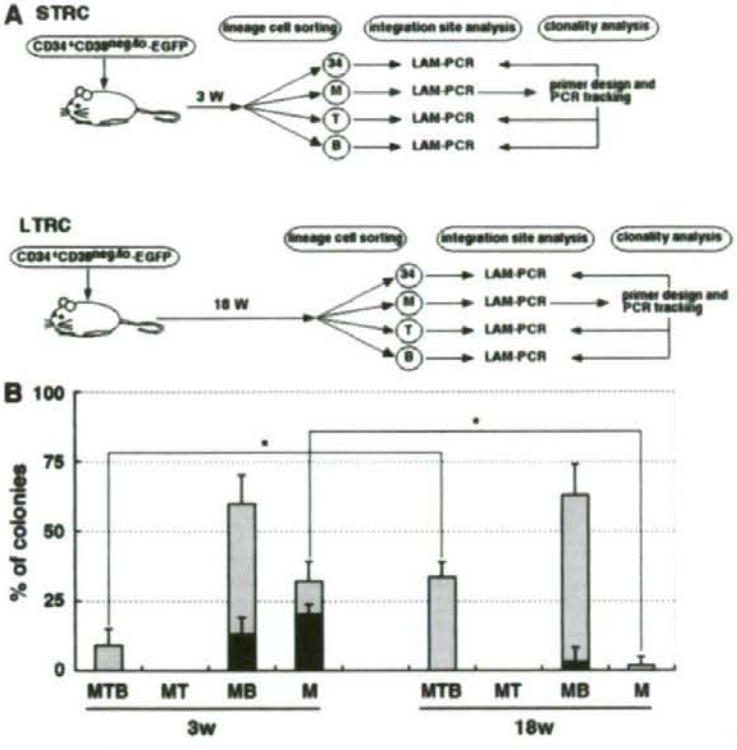

Figure 2. Differentiation ability and self-renewal capacity of individual severe combined immunodeficient mouse-repopulating cell clones. (**A**): Study design for clonal analysis of STRC and LTRC activity. (**B**): Relative frequencies of each clone type. Gray areas in each bar represent the clones detected in CD34 cells, and black areas represent the clones not detected in CD34 cells. A total of 116 clones were analyzed (supplemental online Table 1). Mean SD of four independent experiments are shown. , p .01. Abbreviations: 34, CD34 stem/progenitor cells; B, CD19 B-lymphoid lineage cells; EGFP, enhanced green fluorescent protein; LAM, linear amplification-mediated; lo, low; LTRC, long-term repopulating cell; M, CD33 myeloid lineage cells; neg, negative; PCR, polymerase chain reaction; STRC, short-term repopulating cell; T, CD3 (spleen) or CD4/CD8 DP (thymus) T-lymphoid lineage cells; W, weeks.

cells were able to continuously reconstitute hematopoiesis in vivo.

Repopulation Dynamics of Individual SRC Clones During Human Hematopoietic Reconstitution Originated from CD34 CD38^{neg} Cells

Next, we dissected out the repopulation dynamics of SRCs derived from the quiescent subpopulations of CD34 CD38^{neg} cells. Following transplantation, NOG recipient mice were sacrificed at several time points, and the engraftment and development of human hematopoietic cells were analyzed. Mice that received CD34 CD38^{neg} cells exhibited high levels of CD45 human hematopoietic cell engraftment at 3 weeks after transplantation (the early phase of repopulation) (supplemental online Fig. 2A). The recipients continued to display high levels of human hematopoietic cell (CD45) and stem/progenitor cell (CD34) repopulation between 9 and 18 weeks (the later phase of repopulation). As expected, the human hematopoietic graft in NOG mice consisted mainly of CD33 myeloid lineage cells at 3 weeks after transplantation, but CD19 B-lymphoid cells outgrew after 9 weeks (supplemental online Fig. 2B).

To clarify the specific stem cell activity of individual SRCs originating from quiescent CD34 CD38^{neg} cells that contribute to various stages of hematopoietic reconstitution, we examined the functional aspects of individual SRC clones using LAM-PCR-based viral integration site analysis (Fig. 2A). Each NOG mouse that received EGFP-transduced CD34 CD38^{neg} population was analyzed at two time points. At each time point, EGFP-expressing human hematopoietic lineage cells were sorted, and the fate of individual SRC clones was examined by clone-tracking analysis. Using primers that were designed on the basis of the genomic sequence information of the CD33 myeloid cell integration site, we traced distribution of each clone among phenotypically distinct populations: CD34 stem/progenitor, T-lymphoid, and B-lymphoid cells (all primer sequences are listed in supplemental online Table 1). Three different clone types were observed at each time point: a multipotent type (MTB), in which insertion sites originally detected in CD33 myeloid cells were also detected in T- and B-lymphoid cell populations; a unipotent progenitor containing exclusively myeloid cells; and a bipotent M/B progenitor. We found that the early phase of hematopoietic reconstitution was mostly attributed to myeloid-restricted clones (Fig. 2B; p .01 compared with later phase of reconstitution). On the other hand, the majority of SRC clones found in the later phase of hematopoiesis were of the multilineage cell-producing type (Fig. 2B; p .01).

We previously reported that the presence or the absence of a common integration site in CD34 stem cell populations indicated the current status of individual SRC clones in terms of their stem cell function [12]. The three clone types were further examined to determine whether they stayed in the CD34 stem cell pool (Fig. 2B). Consistent with our previous observations, the proportion of clones that stayed in the CD34 cell population decreased as the differentiation potential of clones restricted to bipotency or unipotency at 3 weeks, suggesting that initial myeloid-producing STRCs were rapidly exhausted from the CD34 stem cell pool. At 18 weeks, the vast majority of clones (95%) stayed in the CD34 stem cell pool, suggesting the self-replication of virally transduced SRC clones that have the ability to produce both lymphoid and myeloid lineages within the stem cell pool.

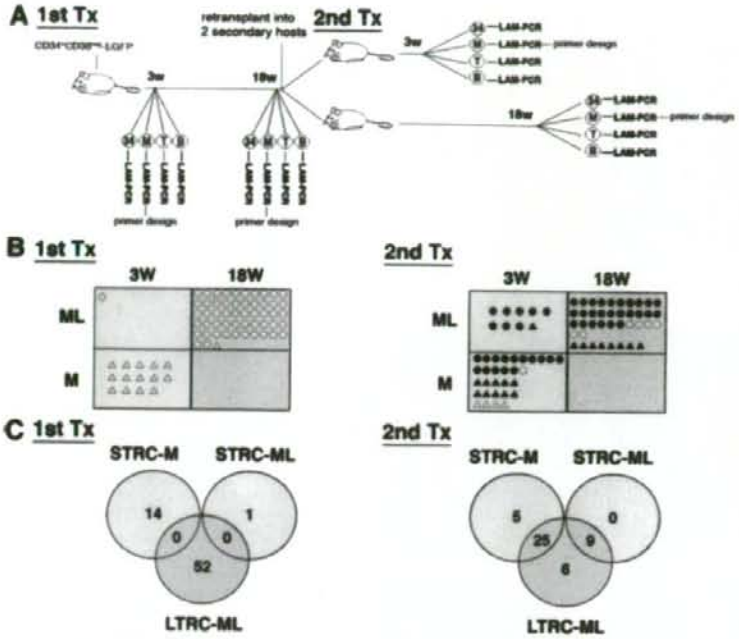

Figure 3. Sequential analysis of individual severe combined immunodeficient mouse-repopulating cell (SRC) clones derived from CD34 $CD38^{neg}$ population. **(A):** Study design for sequential analysis of individual SRC clones. Lineage-specified cells were separated at the indicated time points, and clone-tracking analysis was performed to examine the presence and persistence of specific clones. **(B):** Summary of the sequential clone-tracking analysis from three independent experiments. A total of 112 clones were analyzed (supplemental online Table 2). Open symbols: clones detected at one time point only. Filled symbols: clones simultaneously detected at two time points. Circles: clones detected in the CD34 stem cell pool. Triangles: clones not detected in the CD34 stem cell pool. **(C):** Cumulative number of different types of clones. Numbers in overlapping circles represent clones present at both time points. Abbreviations: B, CD19 B-lymphoid lineage cells; LAM, linear amplification-mediated; LTRC, long-term repopulating cell; M, CD33 myeloid lineage cells; ML, multilineage; PCR, polymerase chain reaction; STRC, short-term repopulating cell; T, CD3 (spleen) or CD4/CD8 DP (thymus) T-lymphoid lineage cells; TX, transplantation; w, weeks.

Sequential SRC Clone-Tracking Analysis Revealed that the Quiescent CD34 $CD38^{neg}$ Cells Constitute the Hierarchical Organization of Human Hematopoiesis

In the recipients of CD34 $CD38^{neg}$ cells, the early phase of repopulation was dominated by myeloid-restricted clones (M-clones), as opposed to the later phase, in which the majority of repopulating clones were multilineage type clones (ML-clones) (Fig. 2B). At this point, it is not clear whether the identical clones produced different types of cells depending on the reconstitution phase or independent clones were responsible for either the early or later phase of repopulation. To find out the origin of repopulating clones in the early and later phases, we performed integration site analysis on individual clones recovered from both phases of the same CD34 $CD38^{neg}$ cell recipient (Fig. 3A, left part; all primer sequences are listed in supplemental online Table 2). At 3 weeks after transplantation, BM cells were aspirated from the tibia of each recipient, and at 18 weeks recipients were sacrificed and BM cells were collected from four long bones. At each time point, EGFP-expressing human hematopoietic lineage cells were sorted for integration site analysis using LAM-PCR. Each proviral integration site serves as a unique marker by which to identify individual clones. When the identical proviral integration site was recognized at different time points, it was regarded as the persistence of the same clone. In that way, we were able to examine the fate of individual SRC clones in the same recipient at different time points. As reported earlier in this study (Fig. 2B), transient M-clones were responsible for the early phase of hematopoietic reconstitution, and self-replicating ML-clones were responsible for the late phase. Interestingly, the transient M-clones detected at the early phase and self-replicating ML-clones were distinctly different (Fig. 3B, 3C, left), indicating that the CD34 $CD38^{neg}$ population, which is highly enriched for human LTRCs, is composed of distinct clonal subsets that are heterogeneous in repopulating kinetics, lineage cell-producing ability, and self-renewal capacity.

To further examine clonal differences in the repopulating cells, we performed clone-tracking analysis on paired secondary transplanted mice. CD34 cells recovered from primary recipients at 18 weeks of transplantation were subsequently transplanted into two secondary recipients, one of which was sacrificed at 3 weeks and the other at 18 weeks after secondary transplantation (Fig. 3A, right). Most of the clones (26 of 38; 68.4%) found in the primary recipients did not engraft in the secondary recipient, suggesting that the repopulating potential of most clones deteriorates during long-term reconstitution in the primary recipient. In contrast, all clones detected in paired secondary recipients had originated from the primary LTRC clones. To our interest, in all the clones found in the secondary recipient pair (a total of 45), there was a significant overlap between STRC and LTRC (34 of 45; 75.6%) (Fig. 3B, 3C, right), which is in contrast to the earlier observation in the primary recipient. This indicates that LTRCs produce both STRCs and LTRCs by asymmetric self-renewal division. It is important to note that although all the STRC-ML clones (9 of 9) demonstrated LTRC activity, some of the STRC-M clones (5 of 30; 16.7%) showed only a transient engraftment, indicating that STRC-M tends to have a more restricted potential than STRC-ML (Fig. 3B, 3C, right). We also identified a small proportion of clones (6 of 45; 13.3%) that were uniquely found in the later phase of secondary repopulation, suggesting the existence of quiescent LTRCs that are reactivated only at the later phase. Taken together, our findings constitute clonal evidence that self-replicating LTRCs produce widely heterogeneous SRC compartments, ultimately constituting hierarchical organization of the human HSC pool (supplemental online Fig. 3).

LTRCs with Higher Self-Renewal Capacity Are Constituted by Relatively Dormant Clones and Expanded Clonally upon Secondary Transplantation

Finally, we quantitatively compared the relative clone size of each LTRC clone that was found in the CD34 stem cell pool of both primary and secondary recipients. Interestingly, all

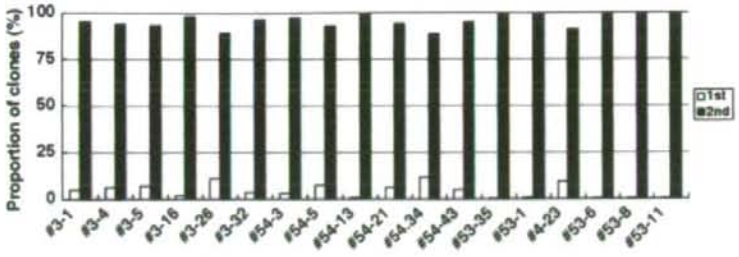

Figure 4. Relative clone size of individual long-term repopulating cell (LTRC) clones in primary and secondary recipients. The clone size of individual LTRC clones detected in CD34 cells was examined by real-time quantitative polymerase chain reaction. The relative clone sizes of each LTRC clone in primary (open bars) and secondary (filled bars) recipients are shown.

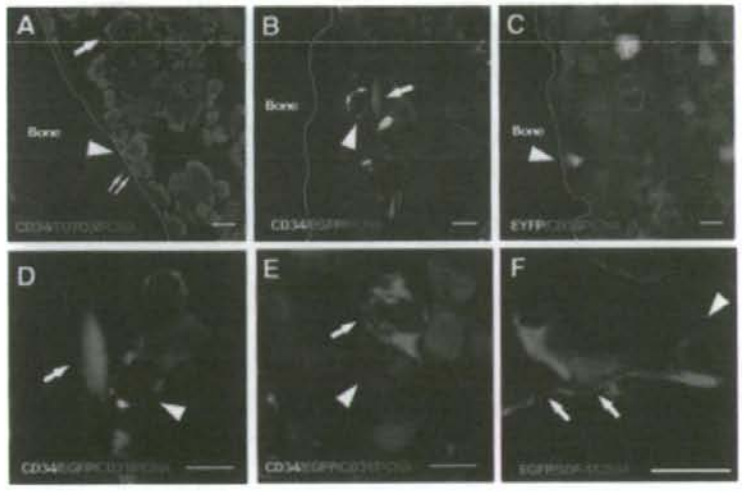

Figure 5. Quiescent human long-term repopulating cells interacting with niche components in the endosteal region. **(A):** Two human CD34 cells, a PCNA-negative (arrowhead) and a PCNA-positive (double arrows), were adjacent to each other and are attached to the endosteum. A large CD34 PCNA-positive cell was found away from endosteum (arrow). **(B):** A PCNA-negative CD34 cell (arrowhead) interacted with CD31-expressing murine endothelial cells (arrow) in the endosteal region. **(C):** The majority of human cells were positive for CD38. A CD38^{low}PCNA-negative EYFP-transduced human cell was attached to the endosteum (arrowhead). **(D, E):** EGFP-marked HMRCs differentiated into fibroblastic reticular cells that associated with CD31 vascular cells. PCNA-negative quiescent CD34 cells (arrowheads) interacted with human reticular cells (arrow). **(F):** HMRCs in the vascular niche expressed SDF-1 (arrows) and interacted with a CD34 cell (arrowhead). Scale bars 10 m. Abbreviations: EGFP, enhanced green fluorescent protein; PCNA, proliferating cell nuclear antigen.

LTRC clones in the CD34 stem cell pool of the secondary recipient were much larger than they had been in the primary recipient (Fig. 4). This suggests that LTRC clones with a higher self-renewal ability are relatively inactive or proliferate slowly, but they could become activated upon secondary transplantation. We also discovered that all quiescent LTRCs were indeed capable of producing multilineage cells in the primary recipients, suggesting that stem cells are not always quiescent but can actively contribute to hematopoiesis when necessary. These results provide evidence for the clonal dynamics of repopulating clones by showing that LTRCs are quiescent at one point and are active at another point.

Quiescent LTRCs Localizes to BM Niches

Maintenance and regulation of LTRCs in vivo depends on the specific microenvironment, known as the niche. We examined the localization of quiescent human CD34 cells in the BM microenvironment of recipients. The quiescent CD34 cells were identified by the lack of PCNA expression. Most of the PCNA CD34 cells (77.8%; n 198 PCNA CD34 cells) were located in the endosteal region (arbitrarily defined as within 12 cells of the endosteum, as described previously [16]) and were found to be associated with bone-lining osteoblasts or endothelial cells (Fig. 5A, 5B). These niche-interacting quiescent human CD34 cells were confirmed as CD38-negative (Fig. 5C), the only cell population transplantable in secondary recipients. In line with previous mouse studies [3–5], these results revealed that human HSCs stayed in a quiescent state to maintain their LTRC activity by actively interacting with the osteoblastic and vascular niche components in the endosteal region of BM.

Mesenchymal Stem Cells Serve As Stem Cells for the Hematopoietic Microenvironment

These experiments had so far demonstrated behavior of human hematopoietic cells in the murine microenvironment. To inspect whether the principles of niche regulatory system extrapolated from murine studies could apply to the human situation, human hematopoietic reconstitution was examined in the "humanized" hematopoietic microenvironment. Previously, we established an experimental system in which a functional human microenvironment was reproduced by the intramedullary injection of human BM MSC-derived HMRCs [15]. The presence of HMRCs was shown to be important in human hematopoietic reconstitution in immunodeficient mice. We examined whether the HMRCs play roles in the maintenance of the LTRC activity in BM. EGFP-transduced human MSCs were intramedullary injected into the right tibia of irradiated NOG mice, and then CD34 cells were transplanted intravenously into each mouse. Consistent with our previous report [15], a majority of HMRCs differentiated into vasculature-associated fibroblastic reticular cells, which are known to play a pivotal role in HSC regulation [17]. In line with this notion, HMRCs expressed one of the important hematopoietic regulatory molecules, SDF-1 (Fig. 5F). Interestingly, the quiescent human CD34 cells often interacted with these EGFP human reticular cells in the endosteal region, strongly suggesting the hematopoiesis-supporting function of these cells (Fig. 5D, 5E). Much to our interest, the number of

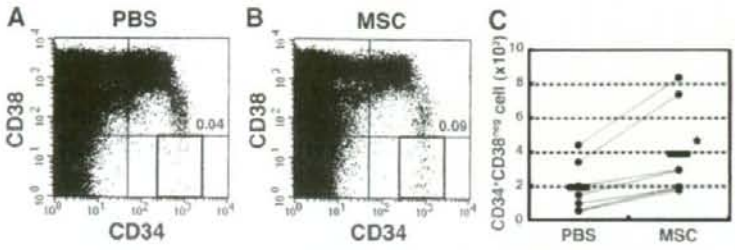

Figure 6. Effect of HMRCs on the engraftment of long-term repopulating cells. **(A):** BM cells obtained from the MSC-injected (right) or PBS-injected (left) tibia from the same mouse were examined by flow cytometry at 12 weeks after transplantation. Representative flow cytometric profiles are shown. The relative frequencies of the CD34 $CD38^{neg}$ population are indicated. **(B):** Absolute numbers of CD34 $CD38^{neg}$ cells in the MSC-injected (right) and the PBS-injected (left) tibias of mice. Each dot represents one mouse. Values obtained from the same mouse are connected with lines. , p .01 relative to the PBS-injected tibia. Abbreviations: MSC, mesenchymal stem cell; neg, negative; PBS, phosphate-buffered saline.

CD34 $CD38^{neg}$ LTRCs in the HMRC-injected tibia was higher than in the saline-injected tibia in the same recipient (Fig. 6). These results confirmed the previous mouse study and demonstrated for the first time that human reticular cells in the endosteal niches were one of the critical components of human LTRC niches.

DISCUSSION

In this study, we demonstrated that the hierarchical organization of human HSCs originated from quiescent CD34 $CD38^{neg}$ cells that resided in the endosteal region of the BM microenvironment, particularly in osteoblastic and vascular niches. Our study presented several lines of evidence that are important in understanding the in vivo dynamics of human hematopoiesis. First, human hematopoiesis was supported by functionally heterogeneous and distinct clonal subsets. Human repopulating cells with predetermined STRC activity contributed to the initial myeloid production, and those clones were rapidly exhausted from the CD34 stem cell pool and lost repopulating ability. In contrast, multilineage-producing LTRC clones remained in the CD34 stem cell pool and sustained hematopoiesis. Asymmetric division of LTRC clones produced clones with different potentials, resulting in the construction of the hierarchical organization of the human HSC pool in the BM microenvironment. Second, repopulating activity of long-lasting LTRCs fluctuated. We quantitatively demonstrated that the self-renewing LTRCs normally stayed in a quiescent state in the primary recipient and expanded clonally upon secondary transplantation. Finally, the hematopoietic microenvironment activity influenced LTRC maintenance. We demonstrated that MSCs served as stem cells for the key components of the hematopoietic microenvironment and that the number of LTRCs could be increased by manipulating microenvironments.

Stem cell quiescence is an indispensable property for the maintenance of hematopoiesis. Interaction of HSCs with their particular microenvironments, known as the stem cell niches, is critical in regulating stem cell quiescence [2]. Although it has been reported that the most primitive human hematopoietic cells, when freshly isolated [18–22], stayed predominantly in the quiescent phase, the cell cycle status and potential of transplanted human HSCs in recipient BM has not been fully examined. In this study, we successfully demonstrated that human LTRCs existed in a rare population of CD34 CD38 cells that localized to the stem cell niches and maintained their stem cell activities while remaining in a quiescent state. Furthermore, we successfully visualized interaction between BM niche cells and a rare population of dormant LTRCs that fulfilled the functional criteria of HSCs: cell cycle quiescence and multilineage engraftment in a secondary host. Combined with our previous finding that showed preferential localization of transplanted CD34 $CD38^{neg}$ cells in the endosteal area [15], the present study indicates that LTRCs protect themselves from extinguishing their stem cell activity by firmly attaching to the endosteal niches in cases of various hematopoietic stresses, as has been demonstrated in mouse studies [23, 24].

Several studies, including the present one, showed that LTRC activity was highly enriched in the CD34 $CD38^{neg}$ fraction, and the self-renewal capacity and differentiation potential of SRCs became restricted, coinciding with the appearance and increasing expression of the CD38 antigen [7–10]. Recently, unexpectedly high repopulating activity was discovered within a CD34 $CD38^{lo}$ subpopulation in direct intrafemoral transplantation experiments [25]. However, the present study demonstrated that CD34 $CD38^{lo}$ cells appeared to be more restricted in their self-renewal ability. Although we were unable to determine the reason for this discrepancy, it is possible that the high self-renewal activity of the CD34 $CD38^{lo}$ subpopulation could be grasped only by direct intrafemoral transplantation. Nevertheless, our experiment has presented the idea that the self-renewal potentials of the CD34 $CD38^{lo}$ and CD34 $CD38^{neg}$ fractions are distinctly different. Furthermore, we demonstrated for the first time that a rare population of CD34 $CD38^{neg}$ cells in the primary recipient BM niches was the only group of SRCs that could successfully reconstitute hematopoiesis in the secondary recipient.

A previous study has reported that in an event that enforces active proliferation of HSCs, such as transplantation, initial active proliferation of SRC population is markedly downregulated after a while [26]. Another study demonstrated an initial upsurge and rapid decline of STRCs in human subjects [27]. Our study showed a similar decline of STRCs. Importantly, our clone-tracking lineage analysis revealed that transient unipotent STRC repopulation was followed by the emergence of multipotent LTRCs. Those LTRCs became activated and produced self-renewing LTRCs and STRCs with limited self-renewal activity. These STRCs in the later phase served as a functional element of the hematopoietic hierarchy. Together with earlier findings, the results of our study provided experimental evidence that quiescent human LTRCs asymmetrically divide in the BM niches, producing one daughter cell that remains in a quiescent state as a "reservoir" of the stem cell pool and another daughter cell that proliferates and differentiates into CD38 cells as a "contributor" for sustaining hematopoiesis.

Several studies in mice and larger animals have concluded that long-term hematopoiesis is sustained by a limited number of self-renewing stem cells that maintain their stem cell activities by staying in a quiescent state and are activated as the occasion demands [28–32]. However, the quantitative dynamics

of individual HSC clones during a quiescent state and an active state remain unclear. In the present study, we quantitatively unveiled that self-renewing LTRC clones normally occupied very small clone size in the primary recipient but expanded remarkably (10–1,000-fold) upon secondary transplantation. Importantly, these quiescent LTRCs were capable of producing multilineage cells even in a steady state in the primary recipients, suggesting that stem cells are not always remained in a quiescent state but can actively contribute to hematopoiesis, depending on the situation.

The exact nature of the HSC niche and the mechanism of HSC regulation have remained largely unknown because of the complex structure of the niche itself and the technical difficulties of examining it. Over the past few years, however, a number of important papers have been published [3–5, 17], and we began to understand how the niche regulates HSCs, at least in mice. Unfortunately, experimental examination of human hematopoietic niches had been hampered by the lack of an appropriate model system until now. We recently established a mouse model that recapitulates a functional human hematopoietic microenvironment [15]. Intramedullary transplanted human MSCs, termed HMRCs, reconstituted functional components of hematopoietic niches. The majority of HMRCs became fibroblastic reticular cells that were often associated with the vasculature, and the rest differentiated into osteoblasts, osteocytes, and endothelial cells. These HMRCs actively interacted with primitive human HSCs to maintain secondary transplantable repopulating activity. Importantly, the HMRCs preferentially distributed to the endosteal region and expressed several niche factors, such as N-cadherin [4], SDF-1 [33–35], and fibronectin [35–37] (T.Y., Y.M., and K.A., unpublished observation). In another published study [35], we demonstrated the important in vivo roles of these niche factors, especially SDF-1, for the engraftment of human HSCs in the BM microenvironment by directly injecting antibody-treated human HSCs into the BM cavity. In the present study, quiescent HSCs interacted with HMRC-derived human reticular cells, and cotransplantation with MSCs resulted in increased engraftment of the CD34 $CD38^{neg}$ population (i.e., the LTRC compartment), emphasizing the importance of the presence of a human microenvironment in an experimental animal. Consistent with our past [15] and present findings, a recent study by Sugiyama et al. elegantly demonstrated that SDF-1-expressing fibroblastic reticular cells play a pivotal role in both osteoblastic and vascular niches at the endosteal region of the murine microenvironment [17]. Taken together, those findings and our own indicated that HMRC-derived fibroblastic reticular cells in the osteoblastic and vascular niches participate in the maintenance of LTRC activity by closely interacting with quiescent human HSCs and secreting hematopoietic-regulatory factors.

Detailed examinations of the innate properties of individual human HSCs that contribute to various phases of reconstitution is important not only to understand human hematopoietic development but also to exploit the therapeutic potential of HSCs. Clinically speaking, rapid recovery of hematopoiesis and sustainable long-term hematopoiesis in patients are primary factors for successful HSC transplantation. In other words, appropriate control of initial hematopoietic recovery and prevention of premature HSC exhaustion could remarkably improve the therapeutic outcome of clinical transplantation. The clonal analysis presented in this study enabled us to accurately evaluate in vivo properties of individual human HSCs. Our strategies may serve as indicators to assess the therapeutic effects of emerging stem cell therapies and help advance clinical transplantation medicine.

CONCLUSION

Through this study, we successfully identified human LTRCs that were responsible for lifelong hematopoiesis in the BM microenvironment. In a steady state, those quiescent human LTRCs localized to and interacted with the key components of the stem cell niche. Once activated, they divided asymmetrically into LTRCs and STRCs, ultimately creating a hierarchical hematopoietic structure. Further identification and characterization of LTRC and STRC subsets will be particularly useful in optimizing protocols for stem cell therapies. Our study also confirmed that MSCs serve as stem cells for the key components of the hematopoietic microenvironment. Therefore, it should be possible to develop MSCs into useful therapeutic tools for conditioning the hematopoietic niches.

ACKNOWLEDGMENTS

We thank members of the animal facility of Tokai University for meticulous care of the experimental animals and members of the Tokai Cord Blood Bank for assistance. We also thank members of the Research Center for Regenerative Medicine of Tokai University for helpful discussion and assistance. This work was supported in part by Grants-in-Aid for Scientific Research from the Ministry of Education, Culture, Sports, Science, and Technology of Japan and by a Research Grant on Human Genome, Tissue Engineering from The Ministry of Health, Labor, and Welfare of Japan.

DISCLOSURE OF POTENTIAL CONFLICTS OF INTEREST

The authors indicate no potential conflicts of interest.

REFERENCES

1 Cheng T, Rodrigues N, Shen H et al. Hematopoietic stem cell quiescence maintained by p21cip1/waf1. Science 2000;287:1804–1808.
2 Wilson A, Trumpp A. Bone-marrow haematopoietic-stem-cell niches. Nat Rev Immunol 2006;6:93–106.
3 Calvi LM, Adams GB, Weibrecht KW et al. Osteoblastic cells regulate the haematopoietic stem cell niche. Nature 2003;425:841–846.
4 Zhang J, Niu C, Ye L et al. Identification of the haematopoietic stem cell niche and control of the niche size. Nature 2003;425:836–841.
5 Kiel MJ, Yilmaz OH, Iwashita T et al. SLAM family receptors distinguish hematopoietic stem and progenitor cells and reveal endothelial niches for stem cells. Cell 2005;121:1109–1121.
6 Shultz LD, Ishikawa F, Greiner DL. Humanized mice in translational biomedical research. Nat Rev Immunol 2007;7:118–130.
7 Bhatia M, Wang JC, Kapp U et al. Purification of primitive human hematopoietic cells capable of repopulating immune-deficient mice. Proc Natl Acad Sci U S A 1997;94:5320–5325.
8 Hogan CJ, Shpall EJ, Keller G. Differential long-term and multilineage engraftment potential from subfractions of human CD34 cord blood cells transplanted into NOD/SCID mice. Proc Natl Acad Sci U S A 2002;99:413–418.
9 Kerre TC, De Smet G, De Smedt M et al. Both CD34 38 and CD34 38- cells home specifically to the bone marrow of NOD/LtSZ scid/scid mice but show different kinetics in expansion. J Immunol 2001;167:3692–3698.
10 Glimm H, Eisterer W, Lee K et al. Previously undetected human hematopoietic cell populations with short-term repopulating activity selec-

tively engraft NOD/SCID-beta2 microglobulin-null mice. J Clin Invest 2001;107:199–206.
11 Guenechea G, Gan OI, Dorrell C et al. Distinct classes of human stem cells that differ in proliferative and self-renewal potential. Nat Immunol 2001;2:75–82.
12 Yahata T, Yumino S, Seng Y et al. Clonal analysis of thymus-repopulating cells presents direct evidence for self-renewal division of human hematopoietic stem cells. Blood 2006;108:2446–2454.
13 Yahata T, Ando K, Nakamura Y et al. Functional human T lymphocyte development from cord blood CD34 cells in nonobese diabetic/Shi-scid, IL-2 Receptor Gamma Null Mice J Immunol 2002;169:204–209.
14 Ito M, Hiramatsu H, Kobayashi K et al. NOD/SCID/gamma(c)(null) mouse: An excellent recipient mouse model for engraftment of human cells. Blood 2002;100:3175–3182.
15 Muguruma Y, Yahata T, Miyatake H et al. Reconstitution of the functional human hematopoietic microenvironment derived from human mesenchymal stem cells in the murine bone marrow compartment. Blood 2006;107:1878–1887.
16 Nilsson SK, Johnston HM, Coverdale JA. Spatial localization of transplanted hemopoietic stem cells: Inferences for the localization of stem cell niches. Blood 2001;97:2293–2299.
17 Sugiyama T, Kohara H, Noda M et al. Maintenance of the hematopoietic stem cell pool by CXCL12-CXCR4 chemokine signaling in bone marrow stromal cell niches. Immunity 2006;25:977–988.
18 Jordan CT, Yamasaki G, Minamoto D. High-resolution cell cycle analysis of defined phenotypic subsets within primitive human hematopoietic cell populations. Exp Hematol 1996;24:1347–1355.
19 Hao QL, Shah AJ, Thiemann FT et al. A functional comparison of CD34 CD38- cells in cord blood and bone marrow. Blood 1995;86:3745–3753.
20 Gothot A, van der Loo JC, Clapp DW et al. Cell cycle-related changes in repopulating capacity of human mobilized peripheral blood CD34( ) cells in non-obese diabetic/severe combined immune-deficient mice. Blood 1998;92:2641–2649.
21 Summers YJ, Heyworth CM, de Wynter EA et al. Cord blood G(0) CD34 cells have a thousand-fold higher capacity for generating progenitors in vitro than G(1) CD34 cells. STEM CELLS 2001;19:505–513.
22 Byk T, Kahn J, Kollet O et al. Cycling G1 CD34 /CD38 cells potentiate the motility and engraftment of quiescent G0 CD34 /CD38-/low severe combined immunodeficiency repopulating cells. STEM CELLS 2005;23:561–574.
23 Haylock DN, Williams B, Johnston HM et al. Hemopoietic stem cells with higher hemopoietic potential reside at the bone marrow endosteum. STEM CELLS 2007;25:1062–1069.
24 Arai F, Hirao A, Ohmura M et al. Tie2/angiopoietin-1 signaling regulates hematopoietic stem cell quiescence in the bone marrow niche. Cell 2004;118:149–161.
25 Mazurier F, Doedens M, Gan OI et al. Rapid myeloerythroid repopulation after intrafemoral transplantation of NOD-SCID mice reveals a new class of human stem cells. Nat Med 2003;9:959–963.
26 Cashman J, Dykstra B, Clark-Lewis I et al. Changes in the proliferative activity of human hematopoietic stem cells in NOD/SCID mice and enhancement of their transplantability after in vivo treatment with cell cycle inhibitors. J Exp Med 2002;196:1141–1149.
27 Glimm H, Schmidt M, Fischer M et al. Efficient marking of human cells with rapid but transient repopulating activity in autografted recipients. Blood 2005;106:893–898.
28 Jordan CT, Lemischka IR. Clonal and systemic analysis of long-term hematopoiesis in the mouse. Genes Dev 1990;4:220–232.
29 Abkowitz JL, Persik MT, Shelton GH et al. Behavior of hematopoietic stem cells in a large animal. Proc Natl Acad Sci U S A 1995;92:2031–2035.
30 Laukkanen MO, Kuramoto K, Calmels B et al. Low-dose total body irradiation causes clonal fluctuation of primate hematopoietic stem and progenitor cells. Blood 2005;105:1010–1015.
31 Kuramoto K, Follman D, Hematti P et al. The impact of low-dose busulfan on clonal dynamics in nonhuman primates. Blood 2004;104:1273–1280.
32 McKenzie JL, Gan OI, Doedens M et al. Individual stem cells with highly variable proliferation and self-renewal properties comprise the human hematopoietic stem cell compartment. Nat Immunol 2006;7:1225–1233.
33 Peled A, Petit I, Kollet O et al. Dependence of human stem cell engraftment and repopulation of NOD/SCID mice on CXCR4. Science 1999;283:845–848.
34 Dar A, Kollet O, Lapidot T. Mutual, reciprocal SDF-1/CXCR4 interactions between hematopoietic and bone marrow stromal cells regulate human stem cell migration and development in NOD/SCID chimeric mice. Exp Hematol 2006;34:967–975.
35 Yahata T, Ando K, Sato T et al. A highly sensitive strategy for SCID-repopulating cell assay by direct injection of primitive human hematopoietic cells into NOD/SCID mice bone marrow. Blood 2003;101:2905–2913.
36 Peled A, Kollet O, Ponomaryov T et al. The chemokine SDF-1 activates the integrins LFA-1, VLA-4, and VLA-5 on immature human CD34( ) cells: Role in transendothelial/stromal migration and engraftment of NOD/SCID mice. Blood 2000;95:3289–3296.
37 Prosper F, Stroncek D, McCarthy JB et al. Mobilization and homing of peripheral blood progenitors is related to reversible downregulation of alpha4 beta1 integrin expression and function. J Clin Invest 1998;101:2456–2467.

See www.StemCells.com for supplemental material available online.

Development of Human Graafian Follicles Following Transplantation of Human Ovarian Tissue into NOD/SCID/γcnull Mice

Yukihiro Terada[1], Yumi Terunuma-Sato[1], Tomoko Kakoi-Yoshimoto[1], Hisataka Hasegawa[1], Tomohisa Ugajin[1], Yoshio Koyanagi[2], Mamoru Ito[3], Takashi Murakami[1], Hironobu Sasano[4], Nobuo Yaegashi[1], Kunihiro Okamura[1]

[1]Department of Obstetrics and Gynecology, Tohoku University Graduate School of Medicine, Sendai, Miyagi, Japan;
[2]Viral Pathogenesis Research Center for AIDS, Institute of Viral Research, Kyoto University, Kyoto, Japan;
[3]Central Institute for Experimental Animals, Kawasaki, Japan;
[4]Department of Pathology, Tohoku University Graduate School of Medicine, Sendai, Miyagi, Japan

Keywords
Graafian follicle, human ovarian cortex, NOG mice, ovarian bursa, xenotransplantation

Correspondence
Yukihiro Terada, Department of Obstetrics and Gynecology, Tohoku University School of Medicine, Seryo-machi, Aoba-ku, Sendai, Miyagi 980-8574, Japan.
E-mail: terada@mail.tains.tohoku.ac.jp

Submitted July 8, 2008;
accepted August 25, 2008.

Citation
Terada Y, Terunuma-Sato Y, Kakoi-Yoshimoto T, Hasegawa H, Ugajin T, Koyanagi Y, Ito M, Murakami T, Sasano H, Yaegashi N, Okamura K. Development of human Graafian follicles following transplantation of human ovarian tissue into NOD/SCID/γcnull mice. Am J Reprod Immunol 2008; 60: 534–540

doi:10.1111/j.1600-0897.2008.00653.x

Problem
Transplantation of human ovarian cortex into host mice may permit various kinds of challenges in reproductive medicine. A novel immunodeficient mouse strain (NOD/SCID/γcnull: NOG) has been developed as a host of transplantation of human tissue.

Method of study
Human ovarian cortex was transplanted into various sites of NOG mice and human follicular development was examined by immunohistochemistry.

Results
Transplantation of human ovarian tissue into NOG mice resulted in approximately similar tissue survival and follicle growth as did transplantation into non-obese diabetic-severe combined immunodeficient mice. The human Graafian follicule from NOG mouse expressed the same steroidogenic enzymes as observed in human Graafian follicles, which developed in the human body. The NOG mice's ovarian bursa was better placed for transplantation than the back skin or kidney capsule.

Conclusion
These results represent the successful generation and biological confirmation of the human Graafian follicles from the human ovarian cortex in the NOG mice.

Introduction

Transplantation of human ovarian tissue into immunodeficient mice has been reported to support follicular development of grafted tissue and may provide an alternative means of obtaining human oocytes from ovarian tissue.[1,2] T and B cell-deficient severe combined immunodeficient (SCID) mice and their derivative strains have successfully been used as hosts for transplantation of human tissue, including thymus, bone, and ovary.[3] Among the available strains, the non-obese diabetic (NOD)/SCID strain is generally preferred because of its defects in innate immunity.[3] Antral follicle development has been reported using fresh and cryopreserved human ovarian tissue following transplantation into SCID

American Journal of Reproductive Immunology 60 (2008) 534–540

mice,[4,5] but so far, there has been no evidence that xenografted human ovarian tissue can develop into a mature Graafian follicle. Indeed, the diameter of human antral stage follicles following transplantation into a NOD/SCID mouse ranged between 0.1 and 5.0 mm,[4,6] far short of the 20 mm average diameter of normal, mature human follicles (Graafian follicles), suggesting that their development was arrested at an immature stage. Nonetheless, the possibility that transplantation of frozen-thawed ovarian tissue into an animal host may allow subsequent maturation and collection of matured oocytes offers considerable advantages.

Despite the obvious interest human follicular development and ovulation hold for reproductive medicine, the mechanisms underlying these processes are still poorly understood. As a result, the success rate for assisted reproductive technology remains low. The major reason for this slow progress is the lack of an experimental system in which the development of human primodial follicles into Graafian follicles can be examined.[7,8] Thus, the establishment of a system in which Graafian follicles can develop from human ovarian cortical tissue outside the human body will be useful, not only for the establishment of ovarian banks but also for elucidation of human follicular development.

Several factors may contribute to the observed arrest of follicular development following xenotransplantation. First, although NOD-SCID mice have been reported to be an ideal host, they retain natural killer cell (NK) activity, which can have negative consequences for xenotransplantation.[3] NOD/SCID/γcnull (NOG) mice, which were generated by eight backcross matings of C57BL/6J-/interleukin -2Rγ allelic mutation (γcnull) mice and NOD-SCID mice,[9] possess multiple immunological defects ranging from defects in cytokine production to the functional incompetence of T, B, and NK cells. These features should provide superb conditions for the development of a xenotransplanted graft. Indeed, the success rates for xenografts of human hematopoietic cells[9] and human myeloma cells[10] into host NOG mice are quite promising. Second, the site of transplantation may be an important factor in promoting the maturation of grafted follicles. Although the site of transplantation has been shown to be important for the success of autologous transplantation of human tissue,[11] it is unclear whether or not it affects follicular development of xenografted human ovarian tissue. Transplantation of human ovarian tissue into mice has largely been performed in the back skin, because it is technically easier than transplantation into the kidney capsule or ovarian bursa and allows easy stimulation and monitoring of follicular development.[4] However, it is unknown whether or not other sites of transplantation will permit improved follicular development.

Here, we report the successful generation of human Graafian follicles following transplantation of human ovarian cortex into NOG mice. These follicles possess characteristics of human Graafian follicles, as assessed by the presence of steroidogenic enzymes. We also compared the survival rates and follicular development of ovarian tissue following transplantation into various host tissues in NOG mice and found that the ovarian bursa supports the survival and production of mature Graafian follicles.

Materials and methods

All procedures for collecting human specimens and animal experiments in this study were approved by the Ethics Committee at Tohoku University School of Medicine.

Animals

NOG mice were generated by eight backcross matings of C57BL/6Jγcnull mice and NOD/Shi-scid mice. Female NOG mice and female NOD-SCID mice were maintained in the Central Institute for Experimental Animals (Kawasaki, Japan) and used at 8–10 weeks of age.

Collection of Human Ovarian Cortex

Ovarian cortex tissue was donated following informed, written consent by women undergoing obstetrical/gynecological operations (five caesarean sections, one abdominal myomectomy, all 21–28 years of age). Ovarian tissue was immediately placed in warm phosphate buffered saline medium supplemented with 5 IU/L of follicle stimulating hormone (Fertinome; Serono, ON, Canada) and transported to our facility. Ovarian cortex was cut into small pieces (2 × 2 × 2 mm) and transplanted into immunodeficient mice.

Xenotransplantation and Ovarian Stimulation

The mice were housed in air-filtered isolator cages, and all surgical procedures were performed in the

laminar flow hood. Bilateral ovariectomy was performed under anesthesia by dorsolateral laparotomy. Human ovarian tissue was transplanted in the back skin, kidney capsule, and ovarian bursa in the same host animal. Two pieces of ovarian tissue were placed in each site. After transplantation, the ovarian bursa was closed by suturing with 9-0 nylon. No antibiotics were used. Ten weeks following transplantation, intraperitoneal injection of human menopausal gonadotropin (HMG, Humegon; Organon, Oss, The Netherlands. 5 IU daily) was commenced and continued for 14 days. The mice were killed 12 weeks following transplantation, and human ovarian grafts were retrieved.

Assessment of Follicular Development and Immunohistochemical Studies

For initial observations, ovarian grafts were observed following transplantation under a dissecting microscope. Transplanted grafts were fixed in 4% parformaldehyde, cut into 3-μm thick sections, and mounted on a glass slide. Immunohistochemistry using streptavidin-biotin amplification (Histofine kit; Nichirei, Tokyo, Japan) was performed as previously described.[6] Polyclonal antibody for P450 cholesterol side chain cleavage (P450 scc) was kindly provided by Dr M. Okamoto (Osaka University School of Medicine, Osaka, Japan), and 3β-hydroxysteroid dehydrogenase (3β-HSD) polyclonal antibody was purchased from Oxygene (Dallas, TX, USA). P450 17α hydroxylase (P450 c17) polyclonal antibody was kindly provided by Dr J. I. Mason (University of Texas, Dallas, TX, USA), and polyclonal antibody for P450 aromatase (P450 arom) was kindly provided by Dr N. Harada (Fujita-Gakuen Health University, Toyoake, Japan). Estrogen receptor (ER) monoclonal antibody was purchased from Immunotech (ERID5; Marseilles, France). Ovarian follicles were classified based on the criteria of Clemont.[12]

Experiment 1

To evaluate the suitability of NOD-SCID and NOG mice as hosts for transplantation of human ovarian tissue, human ovarian cortex from four donors were transplanted into the back skin or ovarian bursa of NOD-SCID ($n = 10$) and NOG mice ($n = 10$). Before transplantation, bilateral ovariectomy was performed under anesthesia by dorsolateral laparotomy, and ovarian tissues were placed in each site. After transplantation, the ovarian bursa was closed by suturing with 9-0 nylon. No antibiotics were used. Ten weeks after transplantation, HMG was administered for 2 weeks, and the survival rates and development of human follicles were compared.

Experiment 2

The effect of transplantation site was determined by transplanting human ovarian tissue from four donors into the back skin, kidney capsule, and ovarian bursa of 25 NOG mice. Each mouse received two grafts in each of the three locations. Ten weeks after transplantation, HMG was administered for 2 weeks, and the survival rates and development of human follicles were compared.

Statistics

The chi-square test was applied to compare the number of follicles found in each graft sample. $P < 0.01$ was considered statistically significant.

Results

Experiment 1

Human ovarian tissue from four donors was transplanted in the back skin of NOD-SCID and NOG mice. Two pieces of donor tissue were transplanted into each mouse, with 10 host mice used for each strain. The tissue survival rate after transplantation was 80% (16/20) for NOD-SCID mice and 90% (18/20) for NOG mice. To examine whether follicle growth occurred in ovarian tissue transplanted into the back skin of NOD-SCID mice, the surviving grafts were sectioned and the central section of each graft was analyzed for follicular development. Five pre-antral follicles were observed in the sections taken from the 16 surviving grafts, and growth of follicles past the pre-antral stage was not observed. Grafts placed into the back skin of NOG mice were similarly analyzed. Five pre-antral follicles and five antral follicles with follicular cavities were observed in the sections taken from the 18 surviving grafts. Total number of antral follicle in the human ovarian tissue transplanted into NOG mice was significantly higher than that was transplanted into NOD-SCID mice (Table I).

Next, human ovarian tissue from four donors was transplanted in the ovarian bursa of NOD-SCID mice

American Journal of Reproductive Immunology 60 (2008) 534–540

Table I Survival and Follicular Development in the Human Ovarian Graft after Transplantation into the Back Skin of the Immunodeficient Mice

Mice strain (number of animals)	Ovarian grafts transplanted	Ovarian grafts survived*	Pre-antral follicle*	Antral follicle*
NOG	20	18[a]	5[b]	5[c]
NOD-SCID	20	16[a']	5[b']	0[c']

*The human ovarian tissue was examined after 2 weeks of human menopausal gonadotropin administration beginning 10 weeks after transplantation. Follicular growth was observed in a central section of a randomly selected graft.
a versus a', b versus b': not significant.
c versus c': $P < 0.05$.

Table II Survival and Follicular Development in the Human Ovarian Graft after Transplantation into the Kidney Capsule of the Immunodeficient Mice

Mice strain	Ovarian grafts transplanted	Ovarian grafts survived*	Pre-antral follicle*	Antral follicle*
NOG	20	18[a]	5[b]	4[c]
NOD-SCID	20	16[a']	4[b']	3[c']

*The human ovarian tissue was examined after 2 weeks of human menopausal gonadotropin administration beginning 10 weeks after transplantation. Follicular growth was observed in a central section of a randomly selected graft.
a versus a', b versus b', c versus c': not significant.

or NOG mice. Each of the 10 mice received two tissue grafts. The tissue survival rate after transplantation was 80% (16/20) in NOD-SCID mice and 90% (18/20) in NOG mice. To examine whether follicle growth occurred in ovarian tissue transplanted into the ovarian bursa of NOD-SCID mice, the surviving grafts were sectioned and the central section of each graft was analyzed for follicular development. Four pre-antral follicles and three follicles that had developed past the antral stage were observed in the sections taken from the 16 surviving grafts. Grafts transplanted into the ovarian bursa of NOG mice were similarly analyzed. Five pre-antral follicles and four antral follicles with follicular cavities were observed in the sections taken from the 18 surviving grafts. No significant difference was found in tissue survival rate and number of developed follicles between NOG mice and NOD-SCID mice (Table II).

Experiment 2

Human ovarian tissue from four donors was transplanted into NOG mice by placing two grafts into each of the following sites: the back skin, kidney capsule, and ovarian bursa. A total of 25 host NOG mice were used. Tissue survival rates after transplantation into NOG mice were 86% (43/50) in the back

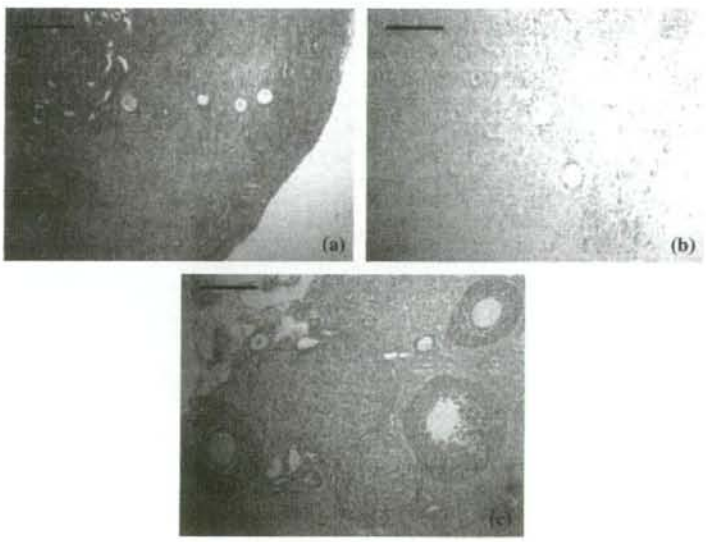

Fig. 1 Histology of human ovarian cortex grafts after transplantation into the back skin (a), kidney capsule (b), and ovarian bursa (c) of the same NOG mouse. More follicles developed in grafts placed in the ovarian bursa than in the back skin or kidney capsule. Scale bar = 200 μm.

Table III Survival and Follicular Development in the Human Ovarian Graft after Transplantation into Transplanted into Back Skin, Kidney Capsule and Ovarian Bursa of the Same NOG Mouse

Site of transplantation	Ovarian grafts transplanted	Ovarian grafts survived	Pre-antral follicle*	Antral follicle*	Graafian follicle*
Back skin	50	43^{a}	8^{b}	6^{c}	0^{d}
Kidney capsule	50	$44^{a'}$	$8^{b'}$	$5^{c'}$	$0^{d'}$
Ovarian bursa	50	$46^{a''}$	$23^{b''}$	$16^{c''}$	$2^{d''}$

*The human ovarian tissue was examined after 2 weeks of human menopausal gonadotropin administration beginning 10 weeks after transplantation. Follicular growth was observed in a central section of a randomly selected graft.
a versus a' versus a'', b versus b', c versus c', d versus d' versus d'': not significant.
b versus b'', b' versus b'', c' versus c'': $P < 0.01$.
c versus c'': $P < 0.05$.

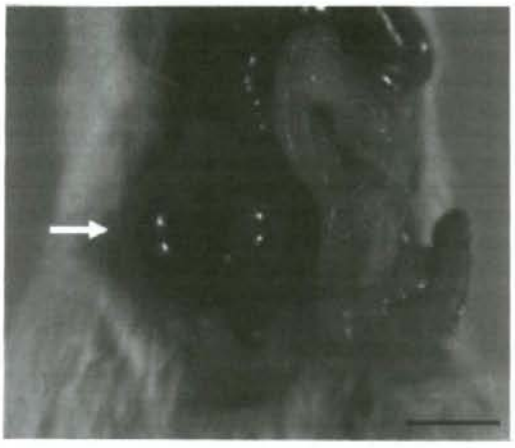

Fig. 2 Macroscopic view of a human Graafian follicle (arrow) after transplantation of human ovarian cortex into the ovarian bursa of a NOG mouse. Host mice were stimulated by daily intraperitoneal injection of human menopausal gonadotropin for 14 days, 10 weeks after transplantation. Scale bar = 1 cm.

skin, 88% (44/50) in the kidney capsule, and 92% (46/50) in the ovarian bursa. To determine whether follicle growth occurred in any of the grafts, they were sectioned and the central section of each graft was analyzed for follicular development (Fig. 1; summarized in Table III). Eight pre-antral follicles were observed in the sections taken from the 43 surviving grafts placed in the back skin, eight from the kidney capsule (out of 44 surviving grafts) and 23 in the ovarian bursa (out of 46 surviving grafts). Six antral follicles with follicular cavities were observed in the 43 surviving grafts placed in the back skin, five in the kidney capsule (out of 44 surviving grafts) and 16 in the ovarian bursa (out of 46 surviving grafts). The total number of human pre-antral and antral follicles developed in human ovarian tissue transplanted into ovarian bursa of NOG mice was significantly higher compared with the number of pre-antral and antral follicles developed in the back skin or kidney capsule of NOG mice (Table III). Graafian follicles (Fig. 2) were observed in two grafts in the ovarian bursa.

Immunohistochemistry

We next used immunohistochemistry to examine the expression of steroidogenic enzymes in human graft-derived Graafian follicles that developed in the ovarian bursa of NOG mice (Fig. 3). P450 scc, P450 c17 (data not shown), and 3β-HSD (data not shown) were localized in the theca cell layer and AD4BP was found in both theca and granulose cells. ER and P450 arom (data not shown) were also detected in the theca cell layer.

Discussion

NOG mice possess multiple immunological defects ranging from dysfunctional cytokine production to functional incompetence of T, B, and NK cells.[9] This combination of defects provides superb conditions for the development of a xenotransplanted graft. To compare the function as the host for xenotransplantation of human ovarian tissue, human ovarian cortex was transplanted into the back skin or ovarian bursa of NOG and NOD-SCID mice and the tissue survival rates and development of human follicles were

American Journal of Reproductive Immunology 60 (2008) 534–540 © 2008 The Authors
Journal compilation © 2008 Blackwell Munksgaard

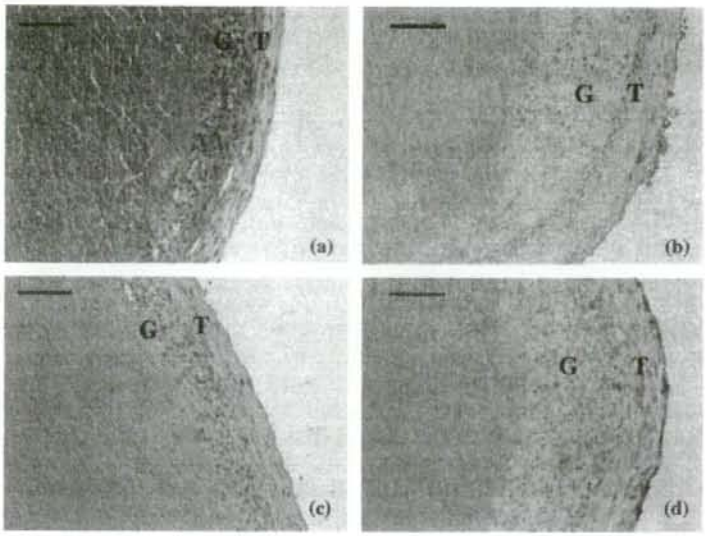

Fig. 3 Characterization of a human Graafian follicle that developed in the ovarian bursa of a NOG mouse (same follicle as shown in Fig. 1). (a) Hematoxylin and eosin staining showing the theca and granulosa cell layers. (b) Antibody staining for the steroidogenic enzyme P450 scc is localized to the cytoplasm of theca cells. (c) Immunohistochemistry for AD4-BP showing expression in the nuclei of both theca and granulosa cell layers. (d) ER antibody staining was detected in the theca cell layer. T, theca cells; G, granulosa cells. Scale bar = 100 μm.

compared. Grafts placed in the ovarian bursa and back skin of NOG mice both showed approximately similar survival rates after transplantation and formed more pre-antral to antral follicles as did ovarian tissue transplantated into NOD-SCID mice (Tables I and II). Development of mature human Graafian follicles (as shown in Fig. 2) was only observed in human ovarian tissue transplanted into the ovarian bursa of NOG mice. From these results, we conclude that NOG mice are better than NOD-SCID mice as a host strain for human ovarian xenografting.

We also examined how the site of transplantation affects the survival rate and follicular development in human ovarian tissue grafted into NOG mice. When human ovarian cortex was transplanted into the back skin, kidney capsule, and ovarian bursa of NOG mice, the most pre-antral or antral follicles developed in the human ovarian tissue, which were transplanted into mices' ovarian bursa. Moreover, in two out of eight transplanted mice, human Graafian follicles (16–18 mm in diameter) were obtained from transplanted tissues within the ovarian bursa (Fig. 2). In contrast, while antral follicles were found in grafts into the back skin or kidney capsule, no Graafian follicles were observed. Thus, the mouse ovarian bursa provides a good microenvironment (e.g. blood flow, kinetics of exogenous gonadotropins, growth factors) for follicular growth and differentiation of grafted human ovarian tissue. However, the reasons for this improved follicular growth and differentiation are still unclear. Interestingly, only one Graafian follicle was formed per graft, suggesting that the mouse ovarian bursa may supply environmental conditions that support the development of single follicles.

We also examined the expression of steroidogenic enzymes in graft-derived follicles by immunohistochemistry. High levels of P450 arom and ER expression were observed in both the granulosa and the theca layer in grafts into the ovarian bursa of NOG mice. The steroidogenic enzymes P450 scc, P450 c17, and 3β-HSD were observed in the cytoplasm of theca cells in antral follicles following xenotransplantation into both NOD-SCID[6] and NOG mice (present study). P450 arom and ER are expressed specifically in Graafian follicles in cycling human ovaries and mark the completion of steroidogenesis in human follicles,[13–15] whereas estrogen plays dual roles in folliculogenesis (via an autocrine system) and oocyte cytoplasmic maturation.[16] P450 arom and ER expression were observed only in the granulosa and theca cell layer in human Graafian follicles that formed in the ovarian bursa of NOG mice (Fig. 3). Thus, the follicles we observed have characteristics similar to the dominant follicles of a normal, pre-menopausal cycling human ovary.

In summary, we have found that NOG mice are good hosts for xenotransplantation of the human

ovarian cortex and that tissue survival and follicle growth vary with the site of transplantation. Our data provide the biological evidence that Graafian follicles can develop outside the human body. This system will allow us to elucidate the mechanisms of human follicular development, which remain elusive.

Acknowledgment

This work was supported by Japan Society for the Promotion of Science to Y.T.

References

1 Gook DA, Edgar DH, Borg J, Archer J, McBain JC: Diagnostic assessment of the developmental potential of human cryopreserved ovarian tissue from multiple patients using xenografting. *Human Reprod* 2005; 20:72–78.

2 Aubard Y: Ovarian tissue xenografting. *Eur J Obstet Gynecol Reprod Biol* 2003; 108:14–18.

3 Shultz LD, Ishikawa F, Greiner DL: Humanized mice in translational biomedical research. *Nat Rev Immunol* 2007; 7:118–130.

4 Weissman A, Gotlieb L, Colgan T, Jurisicova A, Greenblatt EM, Casper RF: Preliminary experience with subcutaneous human ovarian cortex transplantation in the NOD-SCID mouse. *Biol Reprod* 1999; 60:1462–1467.

5 Gook DA, Edgar DH, Borg J, Archer J, Lutjen PJ, McBain JC: Oocyte maturation, follicle rupture and luteinization in human cryopreserved ovarian tissue following xenografting. *Hum Reprod* 2003; 18:1772–1781.

6 Sato Y, Terada Y, Utsunomiya H, Koyanagi Y, Ito M, Miyoshi I, Suzuki T, Sasano H, Murakami T, Yaegashi N, Okamura K: Immnohistochemical localization of steroidogenic enzymes in human follicle following xenotransplantation of the human ovarian cortex into NOD-SCID mice. *Mol Reprod Dev* 2003; 65:67–72.

7 Hovatta O, Wright C, Krausz T, Hardy K, Winston RM: Human primordial, primary and secondary ovarian follicles in long-term culture: effect of partial isolation. *Hum Reprod* 1999; 14:2519–2524.

8 West ER, Shea LD, Woodruff TK: Engineering the follicle microenvironment. *Semin Reprod Med* 2007; 25:287–299.

9 Ito M, Hiramatsu H, Kobayashi K, Suzue K, Kawahata M, Hioki K, Ueyama Y, Koyanagi Y, Sugamura K, Tsuji K, Heike T, Nakahata T: NOD/SCID/gamma(c)(null) mouse: an excellent recipient mouse model for engraftment of human cells. *Blood* 2002; 100:3175–3182.

10 Miyakawa Y, Ohnishi Y, Tomisawa M, Monnai M, Kohmura K, Ueyama Y, Ito M, Ikeda Y, Kizaki M, Nakamura M: Establishment of a new model of human multiple myeloma using NOD/SCID/gammac(null) (NOG) mice. *Biochem Biophys Res Commun* 2004; 313:258–262.

11 Donnez J, Dolmans MM, Demylle D, Jadoul P, Pirard C, Squifflet J, Martinez-Madrid B, van Langendonckt A: Livebirth after orthotopic transplantation of cryopreserved ovarian tissue. *Lancet* 2004; 364:1405–1410.

12 Clement PB: Histology of the ovary. *Am J Surg Pathol* 1987; 11:277–303.

13 Sasano H, Okamoto M, Mason JI, Simpson ER, Mendelson CR, Sasano N, Silverberg SG: Immunolocalization of aromatase, 17α-hydroxylase and side-chain-cleavage cytochromes P-450 in the human ovary. *J Reprod Fertil* 1989; 85:163–169.

14 Suzuki T, Sasano H, Tamura M, Aoki H, Fukaya T, Yajima A, Nagura H, Mason JI: Temporal and spatial localization of steroidogenic enzymes in premenopausal human ovaries: in situ hybridization and immunohistochemical study. *Mol Cell Endocrinol* 1993; 97:135–143.

15 Suzuki T, Sasano H, Kimura N, Tamura M, Fukaya T, Yajima A, Nagura H: Immunohistochemical distribution of progesterone, androgen and oestrogen receptors in the human ovary steroidogenic enzymes. *Hum Reprod* 1998; 13:1922–1927.

16 Tesarik J, Mendoza C: Nongenomic effects of 17 beta-estradiol on maturing human oocytes: relationship to oocyte developmental potential. *J Clin Endocrinol Metab* 1995; 80:1438–1443.

Exp. Anim. 57(5), 471–477, 2008

—Note—

Establishing EGFP Congenic Mice in a NOD/Shi-scid IL2Rg^{null} (NOG) Genetic Background Using a Marker-Assisted Selection Protocol (MASP)

Hiroshi SUEMIZU, Chie YAGIHASHI, Tomoko MIZUSHIMA, Tomoyuki OGURA, Tomoo ETOH, Kenji KAWAI, and Mamoru ITO

Central Institute for Experimental Animals, 1430 Nogawa, Miyamae, Kawasaki 216-0001, Japan

Abstract: *Severely immunocompromised NOD/Shi-scid IL2Rg^{null} (NOG) mice, which show higher engraftment efficiency, are useful as recipients in xenotransplantation studies. We generated a NOG-enhanced green fluorescent protein (EGFP) transgenic (Tg) mouse (NOG-EGFP) that was introduced the EGFP transgene from the C57BL/6-EGFP Tg mouse using the speed congenic method with a marker-assisted selection protocol (MASP). With this method, the selection of the male with the closest NOG strain type was repeated four times. When human cord blood CD34$^+$ cells were transplanted into NOD/Shi-scid, NOG, and NOG-EGFP mice (N_6), the engraftment efficiency of the NOG-EGFP mice was significantly higher than that of the NOD/Shi-scid mice and was similar to that of the NOG mice. These results suggest that the NOG-EGFP mice, which were generated using the congenic method with MASP, acquired the immunological properties of the NOG mice.*

Key words: *microsatellite marker, NOG mouse, speed congenic*

Previously established techniques of introducing additional genetic changes into transgenic or knockout mice include transgenic methods involving the direct microinjection of fertilized eggs and congenic strategies using extant genetically modified mice. The congenic strategy is the classical method and is easiest to perform, but, backcrossing must be performed for at least seven generations to replace over 99% of the genetic background (99.2% is theoretically replaced), which is extremely time-consuming. One of the fastest ways to introduce additional genetic modification is the marker-assisted selection protocol (MASP) known as the "speed congenic" method. In MASP, the male mouse showing the most complete replacement with the targeted genetic background is selected as the "best" male and is used in the next backcross [11–13]. NOG (formally, NOD.Cg-*Prkdc^{scid} Il2rg^{tm1Sug}*/ShiJic) mice, which were developed by introducing IL2Rg^{null} mutation from C57BL/6-*Il2rg^{tm1Sug}* mice with backcross mating to NOD/Shi-*scid* mice [3], have no lymphocytes (neither T nor B) or natural killer (NK) cells, and have impaired dendritic cell function [4, 7]. Therefore, NOG mice can be used to develop "humanized mice", which possess high levels of human-derived cells or tissues. Because it is difficult to label human cells (e.g. hematopoietic stem cells or neural stem cells) with visible markers, we

(Received 26 July 2007 / Accepted 21 April 2008)

Address corresponding: H. Suemizu, Central Institute for Experimental Animals, 1430 Nogawa, Miyamae, Kawasaki 216-0001, Japan